

Surface saline lakes in the Mediterranean Sea

Elena Terzić¹, Clara Gardiol², and Ivica Vilibić^{1,3}

¹Ruđer Bošković Institute, Bijenička cesta 54, 10000 Zagreb, Croatia

²SeaTech, Ecole d'ingénieurs - Université de Toulon, Toulon, France

³Institute for Adriatic Crops and Karst Reclamation, Split, Croatia

Correspondence: Elena Terzić (eterzic@irb.hr)

Abstract.

In the Levantine basin, it has long been known that salinity can reach a maximum in a thin layer near the surface, particularly during the warm season when summer heating, evaporation, and low mixing prevail. This water mass has been linked to the generation of Levantine intermediate and deep waters, depending on winter heat loss and wind-induced mixing. However, a recent study demonstrated that similar conditions, referred to as ‘surface saline lakes’ (SSLs), can occur as far north as the Adriatic Sea. To investigate this, we analyzed data from Argo profiling floats across all Mediterranean basins, focusing on the upper layers (up to 200 m in depth), where such lakes are known to form. We developed an objective algorithm to detect SSLs within profiles, defining a SSL by a threshold-exceeding salinity gradient at its base. This definition allowed us to estimate SSL depth, SSL temperature and potential density anomaly (*PDA*) gradients at the base, and the Schmidt Stability Index which quantifies the energy needed to mix a SSL. We also ensured the quasi-continuity of Argo profiles throughout the year in our analyses, as SSLs are highly seasonal phenomena. SSLs exhibit minimum or vanishing occurrences between February and April, while peaking between August and October. SSLs were detected in all Mediterranean basins, with the highest prevalence—65–70% of profiles between July and December—occurring in the Levantine basin. During the August–October peak, SSLs exceeded 35% of monthly profiles in each basin, even in the Western Mediterranean, albeit with lower overall salinity levels and SSL variables ranges. These findings underscore the role of atmospheric heat and water exchange in all Mediterranean basins, influencing intermediate and deeper thermohaline properties through wintertime mixing. Despite pronounced interannual and seasonal variability, our analysis of data showed a significant positive trend in SSL depth, accompanied by decreasing thermohaline gradients (temperature, salinity, *PDA*) at SSL bases though the investigated period. The observed changes raise questions about their drivers—whether they indicate ongoing climate-change-induced salinization and shifts in Mediterranean water mass dynamics, or are merely manifestations of a multi-decadal variability.

1 Introduction

Understanding seawater salinity is crucial when considering the global water cycle and the changes it might undergo with the changing climate. The next decades are expected to result in an increase in salinity due to increased evaporation (IPCC, 2022), also due to the fact that a warming atmosphere might be able to contain more moisture (Durack et al., 2012). With the emergence of autonomous platforms, it has been possible to obtain numerous vertical profiles of basic thermohaline properties, which in

turn enabled a more in-depth understanding of the spatio-temporal dynamics and long-term changes at an unprecedented scale. Potentially, one of the metrics that could monitor such changes over time might be the selection of salinity profiles with highest values at (sub-)surface layers. In this work, such profiles are defined as surface saline lakes, and have been knowingly a present feature inside the Mediterranean Sea, especially in the Levantine basin (Manca et al., 2004; Ozer et al., 2020; Kubin et al., 2019), as well as occasionally in the Adriatic Sea (Mihanović et al., 2021). With increasing salinity, it can be expected to see more and more such profiles over time, provided that the underlying water is dense enough to preserve such vertical shapes at the observing temporal scales.

The Mediterranean Sea has long been defined as a laboratory basin (Robinson and Golnaraghi, 1994) due to its specific bathymetry and complex dynamics and processes that interact at different spatio-temporal scales, in particular in its ultra-oligotrophic eastern part (Malanotte-Rizzoli et al., 2003). It is one of the climate change hot spots (Giorgi, 2006; Tuel and Eltahir, 2020), with increasing warming and salinification rates, especially in the Eastern Mediterranean (Borghini et al., 2014; Kassis and Korres, 2020; Fedele et al., 2022; Aydogdu et al., 2023; Kubin et al., 2023). Sea surface warming rates have in the past 4 decades been 3-4 times higher compared to the global average (Pisano et al., 2020; Pastor et al., 2020), and climate projections predict a continuation of warming and salinization trends (Soto-Navarro et al., 2020), which could in turn affect the dense water formation efficiency (Somot et al., 2006; Parras-Berrocal et al., 2023; Verri et al., 2024).

The basin's thermohaline circulation follows a cyclonic pattern with numerous (sub-)mesoscale features (Millot and Taupier-Letage, 2005; Malanotte-Rizzoli et al., 2014). Less saline surface water flows from the Atlantic Ocean through the Gibraltar Strait due to the net freshwater deficit of the Mediterranean Sea, where evaporation surpasses precipitation, thus bringing surface salinities to extremely high values (up to and above 39). The Atlantic Water eastward flow in its journey undergoes a gradual increase in temperature and salinity. Upon reaching the easternmost part of the Mediterranean Sea, the Levantine Surface Water, due to its extremely high surface salinity contributes to the formation of Cretan and Levantine intermediate waters (CIW, Velaoras et al., 2014; LIW, Malanotte-Rizzoli et al., 2003). Both of them are involved in the subsequent formation of deep water located in the Eastern Mediterranean, the Adriatic and Aegean Seas, but also reaching as far as the Western Mediterranean in the Gulf of Lions after crossing the Strait of Sicily (Millot, 2013; Margirier et al., 2020). Intermediate waters eventually form the bulk of the Mediterranean Outflow Water, therefore impacting the global ocean conveyor belt through salinization of intermediate Atlantic layers (Aldama-Campino and Döös, 2020; Ayache et al., 2021).

Dense water formation events usually occur in late winter and early spring at the presence of cold and dry winds, such as bora in the Adriatic (Gačić et al., 2002; Mihanović et al., 2013) and mistral in the Gulf of Lions (Somot et al., 2018; Keller et al., 2024). At all dense water formation sites, the density of these waters is preconditioned by higher sub-surface and intermediate salinity values. Additionally, generation of intermediate and deep waters in the Levantine basin has been preconditioned by a sharp maxima in salinity in the upper hundred or less meters, not documented in other basins, forming the so-called Levantine Surface Water (Kubin et al., 2019; Menna et al., 2022). However, a recent study demonstrated that similar conditions may occur as far north as the Adriatic Sea (Mihanović et al., 2021), with exceptionally high surface salinities driven by very low river discharges preconditioning the events for a year, higher-than-average heat fluxes during summer and early autumn periods, and

60 higher-than-average evaporation minus precipitation rates, while the secondary salinity maximum persists in intermediate (up to a few hundred of meters) layers coming from enhanced LIW and/or CIW horizontal flow.

Such changes might affect and modify the current thermohaline circulation patterns. For example, Li and Tanhua (2020) already documented a slow-down of deep ventilation in the Western Mediterranean, as well as a weakened Adriatic Sea source of ventilation in the Eastern Mediterranean. Moreover, Skliris et al. (2018) demonstrated a 20-30% increase in evaporation rates since the mid-20th century also due to lower precipitation and river discharges, further exacerbating sea surface salinities and cases for changed dense water formation patterns and locations. LIW and CIV have also undergone both warming and salinification in the past decades that are faster than global rates (Schroeder et al., 2017; Potiris et al., 2024), at its formation source as well (Velaoras et al., 2015), the latter being due also to the reduced inflow of Black Sea freshened waters (Mamoutos et al., 2024). Furthermore, climate projections predict an increased stratification globally (IPCC, 2022; Holt et al., 2022; Roch et al., 2023) and in the Mediterranean (Llases et al., 2018), which might further increase surface salinities and make vertical mixing less efficient. All these factors combined may result in an increase in salinity profiles that have higher surface and subsurface values due to a more stable water column and enhanced evaporation rates followed by increased warming, which could in turn modify the dense water formation paradigm, favoring double diffusive processes over convective mixing. Such vertical profiles with exceptionally high surface salinities, hereafter referred as surface saline lakes (SSLs), might be therefore an adequate indicator for the dense water preconditioning. In this work we attempted to characterize such vertical profiles by introducing an objective algorithm to detect SSLs with the use of Argo float data set spanning for more than two decades. The international Argo Program has until 2019 already collected, processed, and distributed globally over two million vertical profiles of temperature and salinity from the upper 2000 meters (Wong et al., 2020). It is therefore a powerful tool in order to obtain comprehensive in-situ observations in locations that are also not so easily accessible. The Mediterranean Sea Argo network (Poulain et al., 2007) has collected data since 2001 with gaps only in the northern and middle Adriatic Sea due to its shallow bathymetry and the Tunisian coast with the Gulf of Gabes (Fig.1). Such a high number of easily accessible vertical profiles in the entire basin enabled to study the spatio-temporal distribution of SSLs for the very first time. We introduce a robust algorithm for their detection and also assess possible changes in the past two decades, highlighting their causes and discussing if the observed trends are due to decadal variabilities or changes induced by a changing climate.

85 2 Methods

2.1 Argo Float and Atmospheric Data

For this analysis, Argo profiling floats were downloaded for the entire Mediterranean Sea since their first deployments more than two decades ago (Fig. 1a). Data were downloaded through the ArgoPy data fetcher (<https://pypi.org/project/argopy/>), lastly accessed on 18 November 2024. The temporal range of acquired profiles is between 12 July 2001 and 18 November 2024. Only solid quality control (QC) profiles were chosen, i.e., QC=1 ("good") and QC=2 ("probably good") in delayed, but also real-time mode in order to include profiles from still active floats. Out of 67.554 profiles in total, 64.809 profiles had a QC=1 (good) and only 2.745 were with QC=2 (probably good), which is around 4% of the entire data set. A few additional conditions were set

with the intention of discarding measurements that were not adequate for the analysis, despite the good QC flag. For example, the first measurement needed to be at a depth shallower or equal to 10 m, as the analysis is primarily focused on surface layers.

Moreover, the first depth quota had to be a positive number and all profiles needed to have measurements reaching at least 200 m. Only acquisitions in ascending mode were taken into consideration, and for the purpose of successful vertical gradients calculation (see next section), an additional condition was set that profiles should have only increasing depth values without any vertical oscillations. Variables of temperature (T [$^{\circ}C$]) and practical salinity (S [-]) were used, from which the potential density anomaly (PDA [kgm^{-3}]) values were obtained with the use of TEOS-10 standards (<https://www.teos-10.org>).

Total heat flux and its components (latent, sensible, shortwave and longwave fluxes) averaged over the Levantine basin (latitude range $33-36^{\circ}$ and longitude range $22-33^{\circ}$) were taken from the ERA5 hourly reanalysis (Hersbach et al., 2023), accessed in 04 April 2025. 2024 daily fluxes anomalies were estimated with respect to the 2002-2024 daily averages.

2.2 Surface Saline Lake Detection Metrics

Surface saline lakes were calculated by setting a few conditions for each profile. SSLs' vertical salinity gradient SG was flagged when it reached a threshold value lower or equal than $SG^{thres} = -0.01 m^{-1}$ within the first 200 m. The maximum depth reaching or surpassing the threshold was then defined as the depth of SG , z_{SG} . Concomitantly, values of temperature (TG) and density (DG) gradients were also stored. Additionally, the Schmidt Stability Index (SSI) was obtained as a proxy for the water column stratification based on the approach in Duka et al. (2021), with the sole difference that the surface areas were not taken into consideration since we dealt with profiles and not surface areas. Therefore, for the scope of this work the equation was modified accordingly as:

$$SSI = g \sum_{i=z_0}^{z_{SG}} (z_i - z_g)(\rho_z - \rho_i)\Delta z_i, \quad (1)$$

where g is the gravitational acceleration in $m s^{-2}$, z_i is the depth at the i -th point (m), z_g is the depth between surface and z_{SG} offset by 5 m (m), the ρ_z is the mean density at depth z (kgm^{-3}), ρ_g is the mean density at z_g , Δz_i is the depth between the i -th and $i+1$ -th layer.

Saline lakes needed to meet a few further conditions. For example, salinity at the base of the saline lake had to be lower than the salinity value at the depth closest to the surface for at least 0.05, to avoid SSLs with low surface salinity coming, e.g., from river plumes. In order to reach statistically representative data in temporal terms, certain criteria needed to be met. Firstly, the number of profiles in a year must have been $>1\%$ of the total number of profiles in the whole period per each of the selected regions shown in Fig. 1a. Secondly, the number of profiles in each month of every year needed to be greater than 2% of the total profiles in that year. These percentages were chosen arbitrarily, trying to balance the length of the time series and the availability of enough data for analyses in a particular year or month. The annual number of profiles per each of the selected regions is shown in Fig. 1b.

3 Results

3.1 Upper Layer Climatology

125 Spatially, the collected Argo data was classified into 5 Mediterranean sub-regions, as shown in Fig. 1a: the Western Mediter-
ranean, the Adriatic, Ionian, Aegean seas and the Levantine basin. Climatological median profiles of the upper 200 m of each
of the locations, along with their 10-th and 90-th percentiles, can be seen in Fig. 2. Median temperature profiles range between
18-20°C at the surface and around 14-16°C at 200 m, where the lowest values are found in the Adriatic Sea, while the highest
in the Levantine basin. The 90-th percentile is reaching up to 26°C and 27°C at the surface in all basins and 14.5 and 17°C at
130 200 m in the Western Mediterranean and Levantine basin, respectively. The shallowest thermocline is present in the Adriatic
Sea, presumably as the majority of floats are captured in the quasi-permanent cyclonic Southern Adriatic Gyre where upwelling
is also persistent (Shabrang et al., 2016), while a subsurface temperature maximum can be detected in the Levantine basin. The
median salinity profile exhibits highest values at the first 50 m in the Levantine basin, with values above 39.0 and reaching
more than 39.2 at the very surface (90-th percentile above 39.5). The spatially aggregated profile's vertical shape (median and
135 the percentiles alike) exhibits a typical surface saline lake profile, therefore signifying their ubiquitous presence in the Levan-
tine basin throughout the entire year. The Aegean Sea displays vertically a quasi-constant median value at around 39.1. This
similarly holds also for the Adriatic Sea, although having lower median salinity values, between 38.8 and 38.9, and exhibiting a
weak (sub)surface salinity minimum. The Ionian Sea and Western Mediterranean show a different vertical pattern, with salinity
values increasing with depth, exhibiting the stronger influence of the Atlantic Water at the surface (Fedele et al., 2022). Median
140 values for the Ionian Sea span between 38.7 at the surface and 39.0 at the bottom, and between 37.8 and 38.5 in the Western
Mediterranean. Maximum surface median *PDA* values are seen in the Adriatic Sea and Levantine basins, respectively, i.e.,
28.1 $kg\,m^{-3}$ and 27.9 $kg\,m^{-3}$, with values reaching 29.0 $kg\,m^{-3}$ at 200 m for all basins. The 90-th percentile at the surface
spans between 28.6 $kg\,m^{-3}$ and 29.1 $kg\,m^{-3}$ for the Western Mediterranean and Adriatic Sea, respectively.

3.2 Case Studies of Surface Saline Lakes

145 As an example of the temporal evolution of thermohaline properties in the Levantine basin, a Hovmöller diagram for the long-
term active WMO=6903269 float is shown in Fig. 3, along with its spatial trajectory color-coded in time (between September
2019 and October 2024). Surface salinities are for the first three years seen to have a seasonal variability with increasing values
during early summer lasting until winter, when surface values are lower than at intermediate depths. Appearance of a surface
salinity maximum is always in late spring, lagging for a month or two after the generation of strong seasonal thermocline. The
150 depths of both thermocline and halocline progressively deepened from ca. 10-20 m at their appearance to a hundred meters
before exhibiting some of vertical mixing in winter, while salinity may surpass 39.3 at the surface. Below the halocline, waters
with lower salinity (around or below 39.0) can be found, indicating remnants of Atlantic Water that may be tracked even to these
farthest sections of the Levantine basin (Fach et al., 2021; Zodiatis et al., 2023). Further below, secondary salinity maximum
can be found, fluctuating between 100 and 300 m, indicating LIW generated in previous winters and spreading horizontally
155 over the basin (Kubin et al., 2019). Since mid-2022, however, there is a persistent SSL-like feature without any significant

convective mixing or water column erosion that would bring surface values down or lower than at intermediate depths. Further, the subsurface salinity minimum is quite weak or nonexistent. This is especially seen in late winter and early spring 2024, where temperature, salinity and PDA are more-or-less constant during the vertical mixing phase up to 300 m depth, i.e. $T=19$ °C, $S=39.3$ and $PDA=28.3$ $kg\,m^{-3}$. Indeed, the 2024 vertical mixing was stronger and reached deeper layers than during previous years, as shown in Fig.4. Looking at daily anomalies for winter 2024, negative values are dominant in January and beginning of February, thus implying surface cooling that in turn causes vertical convection to occur.

Examples of T , S and PDA profiles with their vertical gradients for different SSL cases is shown in Fig. 5. Autumn profiles in the Levantine basin (WMO 6901897, sampling date 28 November 2014) and Western Mediterranean (WMO 6903820, sampling date 15 October 2024), Fig. 5a and Fig. 5b, show deeper and more pronounced vertical salinity gradients. SG values reach less than -0.04 m^{-1} in both cases, with TG values of approx. -0.3 and -0.6 °C m^{-1} and DG values of 0.04 and 0.13 $kg\,m^{-4}$ at the z_{SG} depths of 75.0 m and 39.6 m, respectively. Both examples are shown for a period after months of extensive evaporation and water column stabilization during summer. However, the major difference between these two profiles is in overall salinity values, i.e., the Levantine basin SSL has an approximately 0.8 higher salinity than the Western Mediterranean one. The lower limits of saline lake detection are seen in Fig. 5c for the Ionian Sea example (WMO 6990629, sampling date 02 June 2024) in late spring, when the lakes can start forming during the water column stabilization due to the existence of a strong thermocline and increased evaporation (SG value of -0.011 m^{-1} , barely reaching the threshold value, at a depth of 19.8 m). The Adriatic Sea example shown in Fig. 5d, exhibits a shallow, but strong gradient in late summer (WMO 6903799, sampling date 17 August 2023), reaching SG , TG and DG values up to -0.04 m^{-1} less than -0.8 °C m^{-1} and above 0.2 $kg\,m^{-4}$, respectively, at a depth shallower than 15 m, with surface values surpassing 39.2 , in accordance with findings from Mihanović et al. (2021).

3.3 Surface Saline Lakes Climatology

A spatial gradient can be seen in the distribution of SSLs, increasing in percentage towards east (Fig. 6). In the Eastern Mediterranean (the Levantine and Aegean seas), SSLs are present throughout the entire year, with a highest percentage in the Levantine (up to 72% in October). On the other hand, SSLs are reduced in numbers after convective mixing during winter/early spring or completely disappear in the Western Mediterranean, where the highest percentage does not reach a number higher than 35% in September. Overall, a highest percentage is seen in late summer and early autumn months after having reached a longer period of stable stratification and enhanced evaporation, peaking in September/October for most basins. The percentage of SSLs is in general highest in the easternmost region - the Levantine basin, above 40% from June to December, followed by the Adriatic, Ionian and Aegean seas and the Western Mediterranean.

Monthly climatology of surface saline lakes depth, z_{SG} , displays overall lowest values in the Adriatic Sea (except in March) and the Western Mediterranean (except in February), whilst deepest gradient locations are found in the Levantine basin and Aegean Sea (Fig. 7a). Both TG and DG exhibit stronger seasonal variability, clearly showcasing the temperature's influence in determining density in the surface layers. Minimum (maximum) values of TG (DG) can be seen in the Adriatic Sea (between July and September, Figs. 7b, d), denoting shallow but intense accumulation of heat near the surface. Monthly median TG

190 values span between close to zero and $-0.04\text{ }^{\circ}\text{C m}^{-1}$ during summer, reaching peaks in the Adriatic below -0.6 , even $-0.8\text{ }^{\circ}\text{C m}^{-1}$, whereas DG are up to 0.1 and 0.2 kgm^{-4} in the Adriatic. SSI shows greatest values during winter months, similar as in zSG , i.e., up to 1200 Jm^{-2} (Fig. 7e). This might be due to the index's sensitivity to low surface PDA values in the Western Mediterranean which could be caused by an enhanced influence of fresher Atlantic Water. SG , on the other hand, does not show any seasonal variability, with median values ranging between -0.018 and -0.013 m^{-1} , except the Adriatic Sea value on January (Fig. 7d), but this value is based on a limited number of SSLs. High SSI during winter in the Levantine coincides with greatest zSG , therefore showing that certain profiles are not fully eroded during winter cooling and convection, but just stretch SSL towards greater depths (Fig. 7e). On the other hand, in the period between September and December, an increase in zSG is not followed by an increase in SSI . Hence, even though an increase in zSG could be present, the density decrease and changes within a SSL could be the prevailing mechanism for these particular months, which could be due to a higher precipitation rate, riverine discharge, advection of water masses, all of which can cause lower SSI values. The overall median ranges for individual basins are: from $-0.21\text{ }^{\circ}\text{C m}^{-1}$ (Levantine) to $-0.46\text{ }^{\circ}\text{C m}^{-1}$ (Adriatic) for TG , between 0.04 (Levantine) to 0.11 (Adriatic) kgm^{-4} for DG and between 31.6 (Adriatic) to 100 Jm^{-2} (Ionian) for SSI .

Probability density functions (PDFs) for each of the SSL detection and description parameters per region can be seen in Fig. 8. zSG peaks at 20 m in the Adriatic Sea, 35 m in the Western Mediterranean, while around 45 m in other basins. The widest spread is in the Aegean Sea, with high PDF values to depths of approx. 75 m . This might indicate a difference in SSLs between northern and southern Aegean Sea, as the profiles are quite rare in the separation area in the central Aegean Sea populated with a number of islands (Fig. 1a). Unlike for zSG , TG displays a widest spread of PDF in the Adriatic Sea (Fig. 8) and its shape differs substantially compared to other basins, showing a more evenly distributed range of values. In all basins the peak is at slightly lower or around $-0.1\text{ }^{\circ}\text{C m}^{-1}$. In terms of SG , the PDFs do not differ much from basin to basin, all of them peaking at near -0.015 m^{-1} and having a relatively narrow distribution range. As seen in Fig. 7, DG is more influenced by TG , hence the PDF is also more variable between regions, with the Adriatic Sea again having a much wider spread and a flatter peak. This is followed by the Western Mediterranean, whereas the Levantine basin, Ionian and Aegean seas all peak around 0.02 kgm^{-4} and have a very similar distribution shape. SSI shows a flattest distribution range for the Aegean Sea, followed by the Western Mediterranean. The Adriatic and Ionian seas display most similar curves, with the Ionian region peaking at higher SSI values compared to the former. The narrowest PDF is observed for the Levantine basin.

3.4 Interannual variability and trends

Monthly median time series exhibit a high variability between basins (Fig. 9). The Adriatic Sea displays overall lowest (highest) TG (DG) and zSG values, most notably so since 2015, with a continuous decrease (increase) of TG (DG) with time up to present. The Levantine basin, the Aegean and Adriatic seas show a deepening of zSG since 2015, highlighting a drastic jump between 2014 and 2015 (maximum values increasing from 90 to 175 m for the Levantine basin). This shift is concomitant with an increase in SSI , also peaking between 2015 and 2021, after which the values are returning back to the previous or a bit higher range of values up until present.

Due to temporal gaps when looking at each region separately, trends were obtained for the whole Mediterranean Sea (Fig.10). The seasonal signal was removed with annual and semi-annual cosine function fit. Results reveal a deepening of SSLs in time, with zSG increasing around 1 m/year. Vertical gradients of thermohaline properties all exhibit a decreasing trend: SG around $0.0002\ m^{-1}$ per year, $TG = 0.0045\ ^{\circ}C\ m^{-1}$ per year and $DG = -0.0013\ kgm^{-4}$ per year (Fig. 10). SSI has a statistically insignificant increasing trend ($p>0.01$) of $4.81\ Jm^{-2}$ per year, with an interannual dynamic like the one documented for zSG .

3.5 Surface Saline Lake Spatial Extent

Given the way Argo floats measure profiles point-by-point, it is difficult to give a detailed assessment of the spatial extent over which SSLs are present. However, it is possible to give a rough idea by analyzing spatial maps of all float trajectories for certain months, as shown in Fig.11. Four maps were selected for two different years, 2016 and 2021, and for two different months per each of the examined years: one when we have few SSLs (April, Fig.11a and c) and the other when we have the highest percentage of SSLs overall (September/October, Fig.11b and d). Blue dots show profiles where we don't have SSLs, whereas red dots are the ones with SSLs for that specific month and year. April months of 2016 and 2021 display separate and spatially isolated cases of SSLs both east and west, seldom being a part of a series of float samplings, as they only start to emerge with the water column stratification (unless deep enough to have resisted the winter convective mixing). Looking at the two figures in September 2016 and 2021, there is clearly a wider spatial extent and a series of samplings that all correspond to SSLs, hence there is also a wider spatial distribution, often resulting in longer trajectories.

4 Discussion

For the first time, an objective analysis of in situ ocean data indicates that the accumulation of salt near the sea surface during strong heating, evaporation and low mixing seasons is present in the whole Mediterranean Sea. Inside the Mediterranean itself, such salinity profiles have been insofar substantially seen only in the Levantine basin (Manca et al., 2004; Ozer et al., 2020; Kubin et al., 2019), while some case studies document their occasional existence in the Adriatic Sea (Mihanović et al., 2021). The accumulation shows some common characteristics (e.g., halocline strength) and some differences (e.g., the overall temperature and salinity) between different Mediterranean basins. Their widespread presence in different regions inside the Mediterranean suggests that processes (such as wintertime mixing and double diffusivity) that transport surface salt to intermediate depths, previously limited only to the Levantine area and the Adriatic Sea (Amorim et al., 2024), are proved to exist elsewhere.

Results have shown a large seasonal and spatial variability of surface salt accumulation, but also interannual variations that resulted in small, but statistically significant trends. A west-to-east spatial gradient in both depth and frequency of SSLs may be explained with the differences in atmospheric patterns, as well as in general surface salinity values. The Western Mediterranean is less saline due to its proximity to the Atlantic and therefore stronger effects of less saline Atlantic waters, as well as a higher precipitation rate, higher riverine discharge and lower evaporation. The Eastern Mediterranean (except the Adriatic Sea) is more arid with less freshwater discharge, getting some freshwater input through the Nile delta, but is generally a region with much less precipitation, higher evaporation and less wintertime mixing (Ulbrich et al., 2012), all contributing to higher surface salinities.

In terms of interannual variability, the drastic increase in certain properties that define the SSLs (such as zSG and SSI) since 2015 could highlight a change in the atmospheric forcings in the last years, as it was seen for the heat fluxes in the Levantine basin in 2024. However, results could be biased due to spatio-temporal variable float sampling, as well as by the varying annual number of floats. As shown in Fig. 1b, the annual number of floats drastically increased from 2013 onward, but the "jump" seen in Figs. 9a, d and e appeared only from 2015. The explanation that results might not be biased due to varying sampling rates and profile numbers could be further argued when looking at the case of the Ionian Sea (light brown line in Fig. 1b), where the high increase in the number of profiles in 2024 does not result in an increase in zSG or SSI as in 2015 in the Levantine and Adriatic Seas, and a similar increase in the Aegean Sea following in 2016. The Western Mediterranean does not have any such changes, hence it's a question whether this is the result of localized changes in the eastern Mediterranean basins, where trends in both warming and salinification have been rapidly increasing in the past decades (Aydogdu et al., 2023). For example, this has been seen also in the Cretan Sea, especially since 2017 (Chiggiato et al., 2023). During the last salinification phase since 2017, the high salinity increase extended down to depths below the intermediate layer, and it is not yet clear which implications it might have had or will have in the following years. Consequences have been felt in the Southern Adriatic too, facilitating diffusivity of more saline waters originating from the Levantine basin towards the bottom of the pit (Mihanović et al., 2021; Amorim et al., 2024).

In the regional climate projections, net heat loss is expected to decrease (Soto-Navarro et al., 2020) due to an increase in shortwave, net-long wave and sensible heat loss (Dubois et al., 2012). This could have already started resulting in a weakened convection that was unable to efficiently mix the water column, as seen in the Hovmöller diagram in Fig. 3 in the Levantine basin. Enhanced evaporation and reduced precipitation may both contribute to higher surface salinities, thus requiring more energy for an efficient vertical mixing. This has been already demonstrated as a trend in the Mediterranean Sea (Skirris et al., 2018), and it's expected to continue also in the future (Soto-Navarro et al., 2020). In combination with reduced convective mixing, such features could persist over the entire year without being eroded from one winter season to the next, as it's already the case in subtropical gyres in the Atlantic and Pacific Oceans (Melzer and Subrahmanyam, 2017) and will be further explained below.

SSLs might therefore serve as an additional indicator of climate change, given the fact that an increased stratification (and hence less intense mixing) is to be expected in the future as one of the consequences of continuous warming. According to the Special Report on the Ocean and Cryosphere in a Changing Climate (IPCC, 2022), the global stratification has increased in 1998-2019 compared to 1979-1990 for around 2.3% and might increase up to 12-30% compared to the 1985-2005 reference period at the end of the 21st century (2081-2100) in case of a business-as-usual RCP8.5 scenario. Globally, Cheng et al. (2020) estimated an accelerating increase in average salinity since 1960s for the first 2000 meters (2-4 % per °C of warming). Salinity variations can thus sensitively reflect the net exchange of freshwater between the ocean and the atmosphere. Similar mechanisms were observed in the Adriatic Sea, as demonstrated in Mihanović et al. (2021) - after the thermocline formation, the halocline appears after a few months due to the evaporation of a shallow surface layer. The stronger the warming rate, the greater the thermocline and hence higher evaporation rate, which as a consequence causes higher surface salinities.

290 The Mediterranean Sea is quite specific due to its exceptionally high surface salinities. In case of a global salinification trend, changes in the region may potentially provide a clue about the possible changed thermohaline dynamics in other parts of the world and could thus justify its being denoted as a laboratory region. The question remains whether the currently periodic SSLs may become a (quasi-)permanent feature in the absence of strong winds that could erode the vertical profile.

Outside the Mediterranean Sea, surface saline lakes may be (quasi-)permanent features that are present all year round
295 also in the subtropical high atmospheric pressure zones with high evaporation, low precipitation and low vertical mixing induced by winds. Such cases are present both in the Atlantic and Pacific oceans. For example, two float trajectories in the Northern Pacific (WMO=4903503, <https://fleetmonitoring.euro-argo.eu/float/4903503>) and Southern Pacific Subtropical Gyres (WMO=5905261 <https://fleetmonitoring.euro-argo.eu/float/5905261>), regions of North and South Pacific High pressure systems, both exhibit the SSLs as a permanent feature with stable layers of higher (sub-)surface salinities. They reach less
300 than 100 m in the Southern and more than 200 m in the Northern Gyre, albeit maximum salinities do not surpass 35.3 in the North and 36.4 in the South. The Atlantic may be partially influenced by the intrusion of highly saline waters through the Mediterranean Outflow, although the impact it has on the overall higher salinity of the Atlantic compared to the Pacific has been questioned (Jones and Cessi, 2017). A float in the Northern Atlantic Subtropical Gyre, a region of the Azores High pressure system (WMO=4903739, <https://fleetmonitoring.euro-argo.eu/float/4903739>, upon traveling southward, the surface
305 salinity increases to values up to 36.2, exhibiting a permanent and stable layer of higher subsurface salinities. Similarly, in the Southern Atlantic, the region of the St. Helena High (WMO=6904187, <https://fleetmonitoring.euro-argo.eu/float/6904187>), surface salinity reaches up to 36.6, with a SSL shape stable throughout the entire sampling period. Clearly, no seasonality is seen in such regions, and SSLs persist as a stable, constant feature without being eroded. That is the major difference to the current climate of SSLs in the Mediterranean, which still erode in majority of the basin during wintertime mixing and therefore
310 contribute to the generation of intermediate and deep waters and their ventilation.

This method could be in principle extended to other regions, however it should be noted that the salinities in question in the Mediterranean Sea surpass the ones in the other regions by up to 3 or even 4. Maximum salinities in the Pacific cases were between 35.3 and 36.4, whereas values in the Eastern Mediterranean, as well as exceptionally in the Adriatic Sea, may reach even 39.4-39.5, as shown in Figs. 2 and 3. This is an important difference, showing that even though SSLs might be present
315 in other regions, their sheer existence is not a sufficient condition for a potential sinking and dense water formation, as in the Mediterranean. Still, this might eventually change (at a certain level, presumably not like in the Mediterranean) in oceans in the future climate, as subtropical high systems are also projected to change in space, time and intensity (Cherchi et al., 2018).

Linear trends from a time series built from the Mediterranean Argo data after the seasonal signal removal exhibit weakening vertical gradients of temperature, salinity and *PDA*, while at the same time showing a deepening of the SSLs (increasing
320 *zSG*). This could also be an indicator that the water mass under the SSL is getting saltier and warmer, thus weakening the gradients and enabling an easier expansion of SSLs. One of such examples has been already documented and described in Schroeder et al. (2017), where LIW was shown to get both warmer and saltier at the Sicily Channel at intermediate depths.

Finally, SSLs could for all these reasons be a possible indicator of changing biogeochemical properties and therefore may affect marine life. The first strong appearance of SSLs in the Adriatic in 2017 (Beg Paklar et al., 2020) substantially changed

325 microbial food web, e.g. detouring the abundance of heterotrophic bacteria for several standard deviations from the average values, and changing the composition rates between *Prochlorococcus*, *Synechococcus* and picoeukaryotes. Salinization of the Eastern Mediterranean and Southern Adriatic already resulted in a feedback mechanism which completely switched the oxygen content dynamics in the northern Ionian Sea (Martellucci et al., 2024) between different phases of the Adriatic-Ionian Bimodal Oscillating System known - at least up to present - to drive Adriatic thermohaline and biogeochemical properties
330 (Gačić et al., 2010; Civitarese et al., 2010, 2023; Batistić et al., 2014). In the Mediterranean and globally, projected changes in stratification would decrease dissolved oxygen and primary production (Doney et al., 2014; Richon et al., 2019; Lachkar et al., 2024), undoubtedly having strong effects propagating the signal through the food web. Surface saline lakes might be one of mechanisms fostering such changes.

5 Conclusions

335 In this work we introduced a robust and objective algorithm for the detection of upper-layer profiles in different Mediterranean basins characterized by a quasi-constant maximum in salinity above the pycnocline, referred as surface saline lakes (SSLs). This phenomenon has been known to occur regularly in the Levantine basin and sporadically documented for some others, like the Adriatic Sea. First, we showed different examples of vertical profiles where SSLs were spotted, ranging in gradient strength and depth. The climatological analysis showed highest SSLs percentage and their maximum depth in the Eastern
340 Mediterranean, especially the Levantine basin. Minimum occurrences were seen between February and April, while peaking between August and October.

Lakes were present throughout the entire year in the Eastern Mediterranean, whereas in the Western Mediterranean they disappeared in late autumn or early winter, most likely due to the convective erosion of the water column. These findings underscore the role of atmospheric heat and water exchange in all Mediterranean basins, influencing deeper thermohaline
345 properties through winter mixing.

SSLs were detected in all Mediterranean basins, with the highest prevalence occurring in the Levantine region, i.e., 65–70% of profiles between July and December. During the August–October peak, SSLs exceeded 35% of monthly profiles in each basin, even in the Western Mediterranean, albeit with varying overall salinity levels and SSL variables ranges. By having looked at the monthly climatology of various SSL definition parameters, a small range of variability was observed in salinity
350 gradients at the SSL base, unlike for temperature and density gradients, the latter seemingly influenced more by temperature than salinity. SSL depth monthly values ranged between 25 m during spring and summer months to up to 175 m in late winter, concomitantly with high *SSI* values, showing that certain SSLs are deep enough that are not eroded by winter convection.

Despite pronounced interannual and seasonal variability, our analysis of data showed a significant trend in SSL depth, accompanied by decreasing thermohaline gradients (temperature, salinity, *PDA*) at SSL bases though the investigated period.
355 However, these trends may partly reflect sampling biases due to time-space differences in Argo float coverage, which has been substantial before 2013. The observed changes prompt questions about their underlying causes, as the observation period is still too short to derive any robust conclusions—whether they reflect ongoing climate-change-driven salinization and alterations in

Mediterranean water mass dynamics or simply result from natural decadal variability. In any case, the SSLs may be an indicator of changes within the upper ocean where stratification is globally projected to occur, undoubtedly with substantial effects to biogeochemistry and marine life.

Code availability. Codes are freely available upon request.

Data availability. All data was downloaded through Argopy - a Python library aimed at Argo data users: <https://pypi.org/project/argopy/>

Author contributions. ET: Formal analysis, Methodology, Investigation, Data Curation, Writing - Original Draft, Review and Editing, CG: Formal analysis, Investigation, Data Curation, Writing - Review and Editing, IV: Conceptualization, Methodology, Investigation, Writing - Original Draft, Review and Editing, Supervision, Funding Acquisition

Competing interests. Authors declare that there are no competing interests.

Acknowledgements. To Euro-Argo data providers developers and their great work for making the used products and the data available for research. We'd also like to thank MapPlotter (<https://pypi.org/project/MapPlotter/2.2.0/>) and Basins (<https://pypi.org/project/Basins/>) library developers for their effort in making helpful and visually appealing tools for data visualization and spatial division. Also, we are grateful to Argopy (<https://pypi.org/project/argopy/>) library developers for making the Argo data analysis much easier and user-friendlier. The research has been supported by Croatian Science Foundation through project GLOMETS (Grant IP-2022-10-3064) and incoming mobility scheme for postdoctoral researchers (MOBDOL-2023-12, Elena Terzić), as well as by the Interreg Italy-Croatia project AdriaClimPlus (Grant ITHR0200333). The comments and suggestions raised by two anonymous reviewers are also greatly appreciated.

References

- 375 Aldama-Campino, A. and Döös, K.: Mediterranean overflow water in the North Atlantic and its multidecadal variability, *Tellus A: Dynamic Meteorology and Oceanography*, 72, 1565–1577, <https://doi.org/10.1080/16000870.2018.1565027>, 2020.
- Amorim, F. L. L., Le Meur, J., Wirth, A., and Cardin, V.: Tipping of the double-diffusive regime in the southern Adriatic Pit in 2017 in connection with record high-salinity values, *Ocean Science*, 20, 463–474, <https://doi.org/10.5194/os-20-463-2024>, 2024.
- Ayache, M., Swingedouw, D., Colin, C., and Dutay, J.-C.: Evaluating the impact of Mediterranean overflow on the large-scale Atlantic Ocean circulation using neodymium isotopic composition, *Palaeogeography, Palaeoclimatology, Palaeoecology*, 570, 110–139, <https://doi.org/10.1016/j.palaeo.2021.110359>, 2021.
- 380 Aydogdu, A., Miraglio, P., Escudier, R., Clementi, E., and Masina, S.: The dynamical role of upper layer salinity in the Mediterranean Sea, *State of the Planet*, 1–osr7, 1–9, <https://doi.org/10.5194/sp-1-osr7-6-2023>, 2023.
- Batistić, M., Garić, R., and Molinero, J.: Interannual variations in Adriatic Sea zooplankton mirror shifts in circulation regimes in the Ionian Sea, *Climate Research*, 61, 231–240, <https://doi.org/10.3354/cr01248>, 2014.
- 385 Beg Paklar, G., Vilibić, I., Grbec, B., Matić, F., Mihanović, H., Džoić, T., Šantić, D., Šestanović, S., Šolić, M., Ivatek-Šahdan, S., and Kušpilić, G.: Record-breaking salinities in the middle Adriatic during summer 2017 and concurrent changes in the microbial food web, *Progress in Oceanography*, 185, 102–145, <https://doi.org/10.1016/j.pocean.2020.102345>, 2020.
- Borghini, M., Bryden, H., Schroeder, K., Sparnocchia, S., and Vetrano, A.: The Mediterranean is becoming saltier, *Ocean Science*, 10, 693–700, <https://doi.org/10.5194/os-10-693-2014>, 2014.
- 390 Cheng, L., Trenberth, K. E., Gruber, N., Abraham, J. P., Fasullo, J. T., Li, G., Mann, M. E., Zhao, X., and Zhu, J.: Improved Estimates of Changes in Upper Ocean Salinity and the Hydrological Cycle, *Journal of Climate*, 33, 1035–1038, <https://doi.org/10.1175/JCLI-D-20-0366.1>, 2020.
- Cherchi, A., Ambrizzi, T., Behera, S., Freitas, A. C. V., Morioka, Y., and Zhou, T.: The Response of Subtropical Highs to Climate Change, *Current Climate Change Reports*, 4, 371–382, <https://doi.org/10.1007/s40641-018-0114-1>, 2018.
- 395 Chiggiato, J., Artale, V., Durrieu de Madron, X., Schroeder, K., Taupier-Letage, I., Velaoras, D., and Vargas-Yáñez, M.: Chapter 9 - Recent changes in the Mediterranean Sea, in: *Oceanography of the Mediterranean Sea*, edited by Schroeder, K. and Chiggiato, J., pp. 289–334, Elsevier, ISBN 978-0-12-823692-5, <https://doi.org/10.1016/B978-0-12-823692-5.00008-X>, 2023.
- Civitarese, G., Gačić, M., Lipizer, M., and Eusebi Borzelli, G. L.: On the impact of the Bimodal Oscillating System (BiOS) on the biogeochemistry and biology of the Adriatic and Ionian Seas (Eastern Mediterranean), *Biogeosciences*, 7, 3987–3997, <https://doi.org/10.5194/bg-7-3987-2010>, 2010.
- 400 Civitarese, G., Gačić, M., Batistić, M., Bensi, M., Cardin, V., Dulčić, J., Garić, R., and Menna, M.: The BiOS mechanism: History, theory, implications, *Progress in Oceanography*, 216, 103–156, <https://doi.org/10.1016/j.pocean.2023.103056>, 2023.
- Doney, S., Bopp, L., and Long, M.: Historical and Future Trends in Ocean Climate and Biogeochemistry, *Oceanography*, 27, 108–119, <https://doi.org/10.5670/oceanog.2014.14>, 2014.
- 405 Dubois, C., Somot, S., Calmanti, S., Carillo, A., Déqué, M., Dell'Aquila, A., Elizalde, A., Gualdi, S., Jacob, D., L'Hévéder, B., Li, L., Oddo, P., Sannino, G., Scoccimarro, E., and Sevault, F.: Future projections of the surface heat and water budgets of the Mediterranean Sea in an ensemble of coupled atmosphere–ocean regional climate models, *Climate Dynamics*, 39, 1859–1884, <https://doi.org/10.1007/s00382-011-1261-4>, 2012.

- 410 Duka, M. A., Shintani, T., and Yokoyama, K.: Thermal stratification responses of a monomictic reservoir under different seasons and operation schemes, *Science of The Total Environment*, 767, 144 423, <https://doi.org/10.1016/j.scitotenv.2020.144423>, 2021.
- Durack, P. J., Wijffels, S. E., and Matear, R. J.: Ocean Salinities Reveal Strong Global Water Cycle Intensification During 1950 to 2000, *Science*, 336, 455–458, <https://doi.org/10.1126/science.1212222>, 2012.
- Fach, B. A., Orek, H., Yilmaz, E., Tezcan, D., Salihoglu, I., Salihoglu, B., and Latif, M. A.: Water Mass Variability and Levantine Intermediate
415 Water Formation in the Eastern Mediterranean Between 2015 and 2017, *Journal of Geophysical Research: Oceans*, 126, e2020JC016472, <https://doi.org/10.1029/2020JC016472>, 2021.
- Fedele, G., Mauri, E., Notarstefano, G., and Poulain, P. M.: Characterization of the Atlantic Water and Levantine Intermediate Water in the Mediterranean Sea using 20 years of Argo data, *Ocean Science*, 18, 129–142, <https://doi.org/10.5194/os-18-129-2022>, 2022.
- Gačić, M., Civitarese, G., Miserocchi, S., Cardin, V., Crise, A., and Mauri, E.: The open-ocean convection in the Southern Adriatic: a
420 controlling mechanism of the spring phytoplankton bloom, *Continental Shelf Research*, 22, 1897–1908, [https://doi.org/10.1016/S0278-4343\(02\)00050-X](https://doi.org/10.1016/S0278-4343(02)00050-X), 2002.
- Gačić, M., Borzelli, G. L. E., Civitarese, G., Cardin, V., and Yari, S.: Can internal processes sustain reversals of the ocean upper circulation? The Ionian Sea example, *Geophysical Research Letters*, 37, 2010GL043 216, <https://doi.org/10.1029/2010GL043216>, 2010.
- Giorgi, F.: Climate change hot-spots, *Geophysical Research Letters*, 33, 2006GL025 734, <https://doi.org/10.1029/2006GL025734>, 2006.
- 425 Hersbach, H., Bell, B., Berrisford, P., Biavati, G., Horányi, A., Muñoz Sabater, J., Nicolas, J., Peubey, C., Radu, R., Rozum, I., Schepers, D., Simmons, A., Soci, C., Dee, D., and Thépaut, J.-N.: ERA5 hourly data on single levels from 1940 to present. Copernicus Climate Change Service (C3S) Climate Data Store (CDS), <https://doi.org/10.24381/cds.adbb2d47>, [Accessed 04-04-2025], 2023.
- Holt, J., Harle, J., Wakelin, S., Jardine, J., and Hopkins, J.: Why Is Seasonal Density Stratification in Shelf Seas Expected to Increase Under Future Climate Change?, *Geophysical Research Letters*, 49, e2022GL100 448, <https://doi.org/10.1029/2022GL100448>, 2022.
- 430 IPCC: The Ocean and Cryosphere in a Changing Climate: Special Report of the Intergovernmental Panel on Climate Change, Cambridge University Press, 1 edn., ISBN 978-1-00-915796-4 978-1-00-915797-1, <https://doi.org/10.1017/9781009157964>, 2022.
- Jones, C. S. and Cessi, P.: Size Matters: Another Reason Why the Atlantic Is Saltier than the Pacific, *Journal of Physical Oceanography*, 47, 2843–2859, <https://doi.org/10.1175/JPO-D-17-0075.1>, 2017.
- Kassis, D. and Korres, G.: Hydrography of the Eastern Mediterranean basin derived from argo floats profile data, *Deep Sea Research Part II: Topical Studies in Oceanography*, 171, 104 712, <https://doi.org/10.1016/j.dsr2.2019.104712>, 2020.
- 435 Keller, D., Givon, Y., Pennel, R., Raveh-Rubin, S., and Drobinski, P.: Untangling the Mistral and Seasonal Atmospheric Forcing Driving Deep Convection in the Gulf of Lion: 1993–2013, *Journal of Geophysical Research: Oceans*, 129, e2022JC019 245, <https://doi.org/10.1029/2022JC019245>, 2024.
- Kubin, E., Poulain, P.-M., Mauri, E., Menna, M., and Notarstefano, G.: Levantine Intermediate and Levantine Deep Water Formation: An
440 Argo Float Study from 2001 to 2017, *Water*, 11, 1781, <https://doi.org/10.3390/w11091781>, 2019.
- Kubin, E., Menna, M., Mauri, E., Notarstefano, G., Mieruch, S., and Poulain, P.-M.: Heat content and temperature trends in the Mediterranean Sea as derived from Argo float data, *Frontiers in Marine Science*, 10, 1271 638, <https://doi.org/10.3389/fmars.2023.1271638>, 2023.
- Lachkar, Z., Mehari, M., Paparella, F., and Burt, J. A.: Acceleration of Warming, Deoxygenation, and Acidification in the Arabian Gulf Driven by Weakening of Summer Winds, *Geophysical Research Letters*, 51, e2024GL109 898, <https://doi.org/10.1029/2024GL109898>,
445 2024.
- Li, P. and Tanhua, T.: Recent Changes in Deep Ventilation of the Mediterranean Sea; Evidence From Long-Term Transient Tracer Observations, *Frontiers in Marine Science*, 7, 594, <https://doi.org/10.3389/fmars.2020.00594>, 2020.

- Llasses, J., Jordà, G., Gomis, D., Adloff, F., Macías, D., Harzallah, A., Arsouze, T., Akthar, N., Li, L., Elizalde, A., and Sannino, G.: Heat and salt redistribution within the Mediterranean Sea in the Med-CORDEX model ensemble, *Climate Dynamics*, 51, 1119–1143, <https://doi.org/10.1007/s00382-016-3242-0>, 2018.
- 450 Malanotte-Rizzoli, P., Artale, V., Borzelli-Eusebi, G. L., Brenner, S., Crise, A., Gacic, M., Kress, N., and Marullo, S.: Physical forcing and physical/biochemical variability of the Mediterranean Sea: a review of unresolved issues and directions for future research, *Ocean Sci.*, 2014.
- Malanotte-Rizzoli, P., Manca, B. B., Marullo, S., Ribera D'Alcalá, M., Roether, W., Theocharis, A., Bergamasco, A., Budillon, G., Sansone, E., Civitarese, G., Conversano, F., Gertman, I., Hernt, B., Kress, N., Kioroglou, S., Kontoyannis, H., Nittis, K., Klein, B., Lascaratos, A., Latif, M. A., Ozsoy, E., Robinson, A. R., Santoleri, R., Viezzoli, D., and Kovacevic, V.: The Levantine Intermediate Water Experiment (LIWEX) Group: Levantine basin—A laboratory for multiple water mass formation processes, *Journal of Geophysical Research: Oceans*, 108, 2002JC001643, <https://doi.org/10.1029/2002JC001643>, 2003.
- 455 Mamoutos, I. G., Potiris, E., Androurlidakis, Y., Tragou, E., and Zervakis, V.: Evidence for Reduced Black Sea Water Outflow to the North Aegean, *Earth and Space Science*, 11, e2024EA003674, <https://doi.org/10.1029/2024EA003674>, 2024.
- Manca, B., Burca, M., Giorgetti, A., Coatanoan, C., Garcia, M.-J., and Iona, A.: Physical and biochemical averaged vertical profiles in the Mediterranean regions: an important tool to trace the climatology of water masses and to validate incoming data from operational oceanography, *Journal of Marine Systems*, 48, 83–116, <https://doi.org/10.1016/j.jmarsys.2003.11.025>, 2004.
- Margirier, F., Testor, P., Heslop, E., Mallil, K., Bosse, A., Houpert, L., Mortier, L., Bouin, M.-N., Coppola, L., D'Ortenzio, F., Durrieu De Madron, X., Mourre, B., Prieur, L., Raimbault, P., and Taillandier, V.: Abrupt warming and salinification of intermediate waters interplays with decline of deep convection in the Northwestern Mediterranean Sea, *Scientific Reports*, 10, 20923, <https://doi.org/10.1038/s41598-020-77859-5>, 2020.
- 465 Martellucci, R., Menna, M., Mauri, E., Pirro, A., Gerin, R., Paladini De Mendoza, F., Garić, R., Batistić, M., Di Biagio, V., Giordano, P., Langone, L., Misericocchi, S., Gallo, A., Notarstefano, G., Savonitto, G., Bussani, A., Pacciaroni, M., Zuppelli, P., and Poulain, P.-M.: Recent changes of the dissolved oxygen distribution in the deep convection cell of the southern Adriatic Sea, *Journal of Marine Systems*, 245, 103988, <https://doi.org/10.1016/j.jmarsys.2024.103988>, 2024.
- 470 Melzer, B. A. and Subrahmanyam, B.: Decadal changes in salinity in the oceanic subtropical gyres, *Journal of Geophysical Research: Oceans*, 122, 336–354, <https://doi.org/10.1002/2016JC012243>, 2017.
- Menna, M., Gačić, M., Martellucci, R., Notarstefano, G., Fedele, G., Mauri, E., Gerin, R., and Poulain, P.-M.: Climatic, Decadal, and Interannual Variability in the Upper Layer of the Mediterranean Sea Using Remotely Sensed and In-Situ Data, *Remote Sensing*, 14, 1322, <https://doi.org/10.3390/rs14061322>, 2022.
- Mihanović, H., Vilibić, I., Carniel, S., Tudor, M., Russo, A., Bergamasco, A., Bubić, N., Ljubešić, Z., Viličić, D., Boldrin, A., Malačič, V., Celio, M., Comici, C., and Raicich, F.: Exceptional dense water formation on the Adriatic shelf in the winter of 2012, *Ocean Science*, 9, 561–572, <https://doi.org/10.5194/os-9-561-2013>, 2013.
- 480 Mihanović, H., Vilibić, I., Šepić, J., Matić, F., Ljubešić, Z., Mauri, E., Gerin, R., Notarstefano, G., and Poulain, P.-M.: Observation, Preconditioning and Recurrence of Exceptionally High Salinities in the Adriatic Sea, *Frontiers in Marine Science*, 8, 672210, <https://doi.org/10.3389/fmars.2021.672210>, 2021.
- Millot, C.: Levantine Intermediate Water characteristics: an astounding general misunderstanding!, *Scientia Marina*, 77, 217–232, <https://doi.org/10.3989/scimar.03518.13A>, 2013.

- 485 Millot, C. and Taupier-Letage, I.: Circulation in the Mediterranean Sea, in: *The Mediterranean Sea*, edited by Saliot, A., vol. 5K, pp. 29–66, Springer Berlin Heidelberg, Berlin, Heidelberg, ISBN 978-3-540-25018-0 978-3-540-31492-9, <https://doi.org/10.1007/b107143>, series Title: Handbook of Environmental Chemistry, 2005.
- Ozer, T., Gertman, I., Gildor, H., Goldman, R., and Herut, B.: Evidence for recent thermohaline variability and processes in the deep water of the Southeastern Levantine Basin, *Mediterranean Sea, Deep Sea Research Part II: Topical Studies in Oceanography*, 171, 104651,
490 <https://doi.org/10.1016/j.dsr2.2019.104651>, 2020.
- Parras-Berrocal, I. M., Vázquez, R., Cabos, W., Sein, D. V., Álvarez, O., Bruno, M., and Izquierdo, A.: Dense water formation in the eastern Mediterranean under a global warming scenario, *Ocean Science*, 19, 941–952, <https://doi.org/10.5194/os-19-941-2023>, 2023.
- Pastor, F., Valiente, J. A., and Khodayar, S.: A Warming Mediterranean: 38 Years of Increasing Sea Surface Temperature, *Remote Sensing*, 12, 2687, <https://doi.org/10.3390/rs12172687>, 2020.
- 495 Pisano, A., Marullo, S., Artale, V., Falcini, F., Yang, C., Leonelli, F. E., Santoleri, R., and Buongiorno Nardelli, B.: New Evidence of Mediterranean Climate Change and Variability from Sea Surface Temperature Observations, *Remote Sensing*, 12, 132, <https://doi.org/10.3390/rs12010132>, 2020.
- Potiris, M., Mamoutos, I. G., Tragou, E., Zervakis, V., Kassis, D., and Ballas, D.: Dense Water Formation Variability in the Aegean Sea from 1947 to 2023, *Oceans*, 5, 611–636, <https://doi.org/10.3390/oceans5030035>, 2024.
- 500 Poulain, P.-M., Barbanti, R., Font, J., Cruzado, A., Millot, C., Gertman, I., Griffa, A., Molcard, A., Rupolo, V., Le Bras, S., and Petit de la Villeon, L.: MedArgo: a drifting profiler program in the Mediterranean Sea, *Ocean Science*, 3, 379–395, <https://doi.org/10.5194/os-3-379-2007>, 2007.
- Richon, C., Dutay, J.-C., Bopp, L., Le Vu, B., Orr, J. C., Somot, S., and Dulac, F.: Biogeochemical response of the Mediterranean Sea to the transient SRES-A2 climate change scenario, *Biogeosciences*, 16, 135–165, <https://doi.org/10.5194/bg-16-135-2019>, 2019.
- 505 Robinson, A. R. and Golnaraghi, M.: The Physical and Dynamical Oceanography of the Mediterranean Sea, in: *Ocean Processes in Climate Dynamics: Global and Mediterranean Examples*, edited by Malanotte-Rizzoli, P. and Robinson, A. R., pp. 255–306, Springer Netherlands, Dordrecht, ISBN 978-94-010-4376-2 978-94-011-0870-6, https://doi.org/10.1007/978-94-011-0870-6_12, 1994.
- Roch, M., Brandt, P., and Schmidtko, S.: Recent large-scale mixed layer and vertical stratification maxima changes, *Frontiers in Marine Science*, 10, 1277316, <https://doi.org/10.3389/fmars.2023.1277316>, 2023.
- 510 Schroeder, K., Chiggiato, J., Josey, S. A., Borghini, M., Aracri, S., and Sparnocchia, S.: Rapid response to climate change in a marginal sea, *Scientific Reports*, 7, 4065, <https://doi.org/10.1038/s41598-017-04455-5>, 2017.
- Shabrang, L., Menna, M., Pizzi, C., Lavigne, H., Civitarese, G., and Gačić, M.: Long-term variability of the southern Adriatic circulation in relation to North Atlantic Oscillation, *Ocean Science*, 12, 233–241, <https://doi.org/10.5194/os-12-233-2016>, 2016.
- Skliris, N., Zika, J. D., Herold, L., Josey, S. A., and Marsh, R.: Mediterranean sea water budget long-term trend inferred from salinity
515 observations, *Climate Dynamics*, 51, 2857–2876, <https://doi.org/10.1007/s00382-017-4053-7>, 2018.
- Somot, S., Sevault, F., and Déqué, M.: Transient climate change scenario simulation of the Mediterranean Sea for the twenty-first century using a high-resolution ocean circulation model, *Climate Dynamics*, 27, 851–879, <https://doi.org/10.1007/s00382-006-0167-z>, 2006.
- Somot, S., Houpert, L., Sevault, F., Testor, P., Bosse, A., Taupier-Letage, I., Bouin, M.-N., Waldman, R., Cassou, C., Sanchez-Gomez, E., Durrieu De Madron, X., Adloff, F., Nabat, P., and Herrmann, M.: Characterizing, modelling and understanding the climate variability of
520 the deep water formation in the North-Western Mediterranean Sea, *Climate Dynamics*, 51, 1179–1210, <https://doi.org/10.1007/s00382-016-3295-0>, 2018.

- Soto-Navarro, J., Jordá, G., Amores, A., Cabos, W., Somot, S., Sevault, F., Macías, D., Djurdjevic, V., Sannino, G., Li, L., and Sein, D.: Evolution of Mediterranean Sea water properties under climate change scenarios in the Med-CORDEX ensemble, *Climate Dynamics*, 54, 2135–2165, <https://doi.org/10.1007/s00382-019-05105-4>, 2020.
- 525 Tuel, A. and Eltahir, E. A. B.: Why Is the Mediterranean a Climate Change Hot Spot?, *Journal OF Climate*, 33, 5829–5843, <https://doi.org/10.1175/JCLI-D-19-0910.1>, 2020.
- Ulbrich, U., Lionello, P., Belušić, D., Jacobeit, J., Knippertz, P., Kuglitsch, F. G., Leckebusch, G. C., Luterbacher, J., Maugeri, M., Maheras, P., Nissen, K. M., Pavan, V., Pinto, J. G., Saaroni, H., Seubert, S., Toreti, A., Xoplaki, E., and Ziv, B.: 5 - Climate of the Mediterranean: Synoptic Patterns, Temperature, Precipitation, Winds, and Their Extremes, in: *The Climate of the Mediterranean Region*, edited by Lionello, P., pp. 301–346, Elsevier, Oxford, ISBN 978-0-12-416042-2, <https://doi.org/10.1016/B978-0-12-416042-2.00005-7>, 2012.
- 530 Velaoras, D., Krokos, G., Nittis, K., and Theocharis, A.: Dense intermediate water outflow from the Cetan Sea: A salinity driven, recurrent phenomenon, connected to thermohaline circulation changes, *Journal of Geophysical Research: Oceans*, 119, 4797–4820, <https://doi.org/10.1002/2014JC009937>, 2014.
- Velaoras, D., Krokos, G., and Theocharis, A.: Recurrent intrusions of transitional waters of Eastern Mediterranean origin in the Cretan Sea as a tracer of Aegean Sea dense water formation events, *Progress in Oceanography*, 135, 113–124, <https://doi.org/10.1016/j.pocean.2015.04.010>, 2015.
- 535 Verri, G., Furnari, L., Gunduz, M., Senatore, A., Santos Da Costa, V., De Lorenzis, A., Fedele, G., Manco, I., Mentaschi, L., Clementi, E., Coppini, G., Mercogliano, P., Mendicino, G., and Pinardi, N.: Climate projections of the Adriatic Sea: role of river release, *Frontiers in Climate*, 6, 1368413, <https://doi.org/10.3389/fclim.2024.1368413>, 2024.
- 540 Wong, A. P. S., Wijffels, S. E., Riser, S. C., Pouliquen, S., Hosoda, S., Roemmich, D., Gilson, J., Johnson, G. C., Martini, K., Murphy, D. J., Scanderbeg, M., Bhaskar, T. V. S. U., Buck, J. J. H., Merceur, F., Carval, T., Maze, G., Cabanes, C., André, X., Poffa, N., Yashayaev, I., Barker, P. M., Guinehut, S., Belbéoch, M., Ignaszewski, M., Baringer, M. O., Schmid, C., Lyman, J. M., McTaggart, K. E., Purkey, S. G., Zilberman, N., Alkire, M. B., Swift, D., Owens, W. B., Jayne, S. R., Hersh, C., Robbins, P., West-Mack, D., Bahr, F., Yoshida, S., Sutton, P. J. H., Cancouët, R., Coatanoan, C., Dobbler, D., Juan, A. G., Gourrion, J., Kolodziejczyk, N., Bernard, V., Bourlès, B., Claustre, H.,
- 545 D’Ortenzio, F., Le Reste, S., Le Traon, P.-Y., Rannou, J.-P., Saout-Grit, C., Speich, S., Thierry, V., Verbrugge, N., Angel-Benavides, I. M., Klein, B., Notarstefano, G., Poulain, P.-M., Vélez-Belchí, P., Suga, T., Ando, K., Iwasaka, N., Kobayashi, T., Masuda, S., Oka, E., Sato, K., Nakamura, T., Sato, K., Takatsuki, Y., Yoshida, T., Cowley, R., Lovell, J. L., Oke, P. R., Van Wijk, E. M., Carse, F., Donnelly, M., Gould, W. J., Gowers, K., King, B. A., Loch, S. G., Mowat, M., Turton, J., Rama Rao, E. P., Ravichandran, M., Freeland, H. J., Gaboury, I., Gilbert, D., Greenan, B. J. W., Ouellet, M., Ross, T., Tran, A., Dong, M., Liu, Z., Xu, J., Kang, K., Jo, H., Kim, S.-D., and Park, H.-M.:
- 550 Argo Data 1999–2019: Two Million Temperature-Salinity Profiles and Subsurface Velocity Observations From a Global Array of Profiling Floats, *Frontiers in Marine Science*, 7, 700, <https://doi.org/10.3389/fmars.2020.00700>, 2020.
- Zodiatis, G., Brenner, S., Gertman, I., Ozer, T., Simoncelli, S., Ioannou, M., and Savva, S.: Twenty years of in-situ monitoring in the south-eastern Mediterranean Levantine basin: Basic elements of the thermohaline structure and of the mesoscale circulation during 1995-2015, *Frontiers in Marine Science*, 9, 1074504, <https://doi.org/10.3389/fmars.2022.1074504>, 2023.

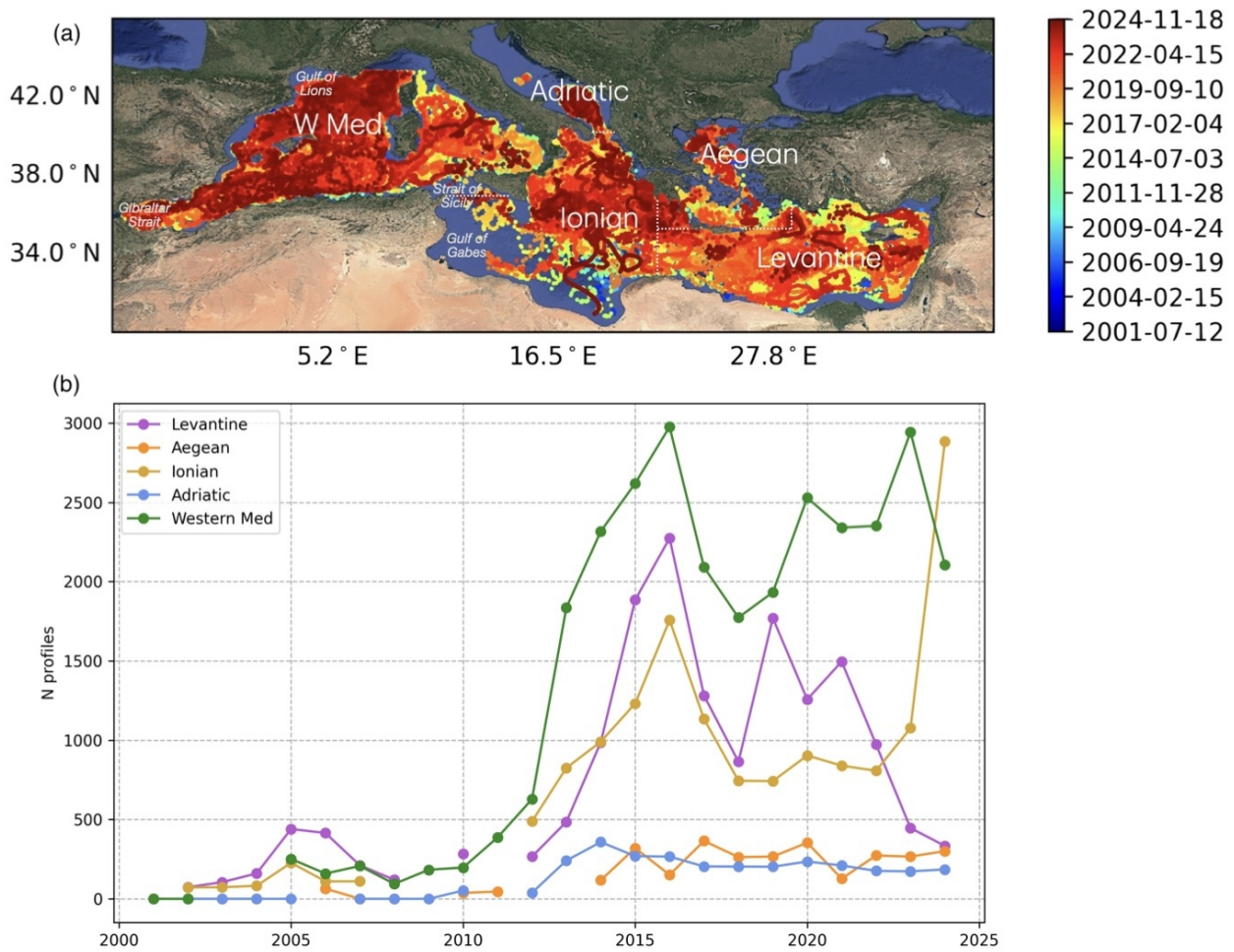


Figure 1. (a) The Mediterranean Sea geography, with color-coded time span of Argo profiles used in the research and marked regions over which the analyses have been carried out: the Adriatic Sea, the Ionian Sea, the Aegean Sea, the Levantine basin and the Western Mediterranean (image background from ©Google Maps). (b) The annual number of of Argo profiles per basin.

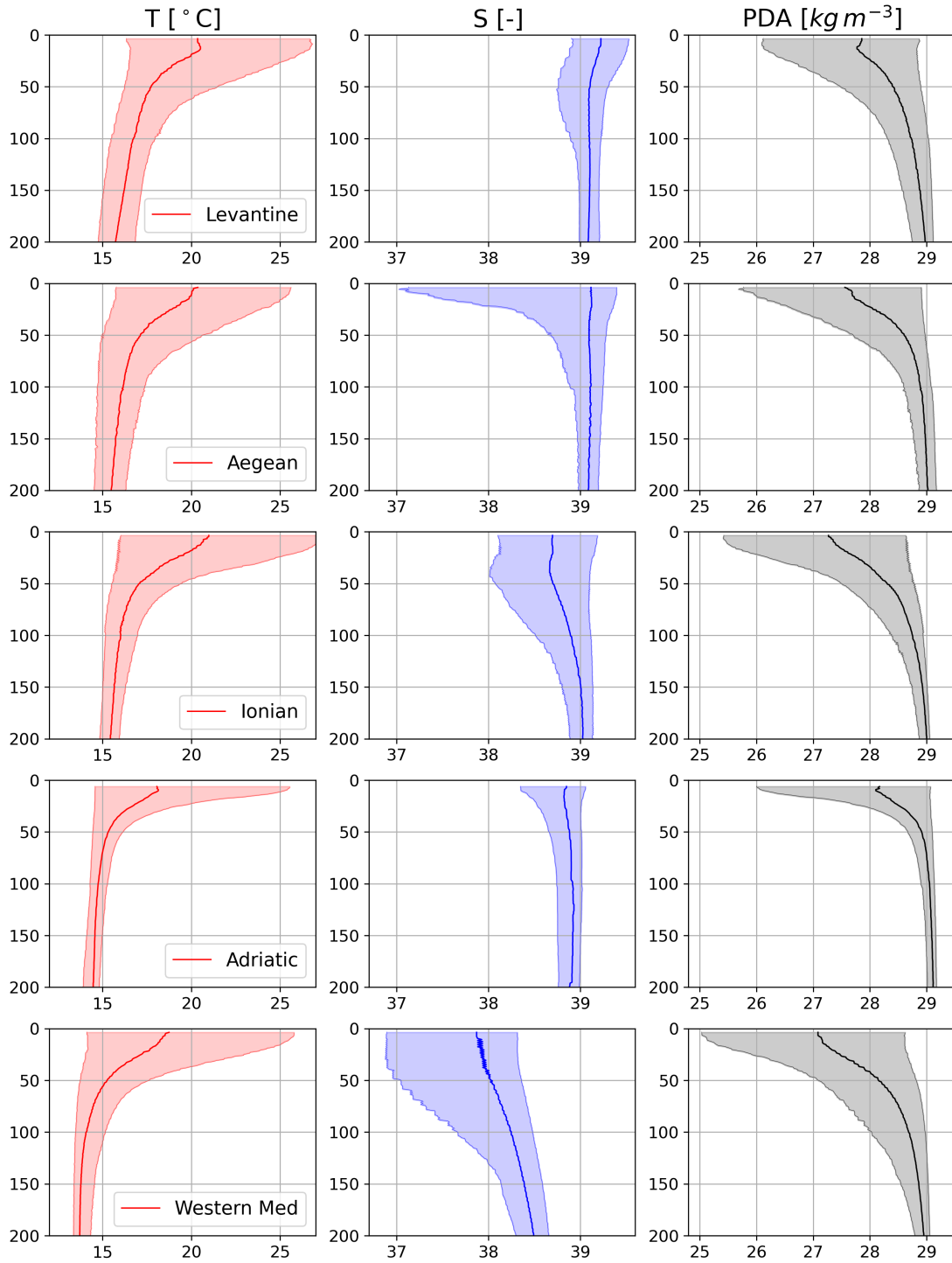


Figure 2. Median values with the 10-th and 90-th percentiles for T, S, PDA (columns) per basin (rows).

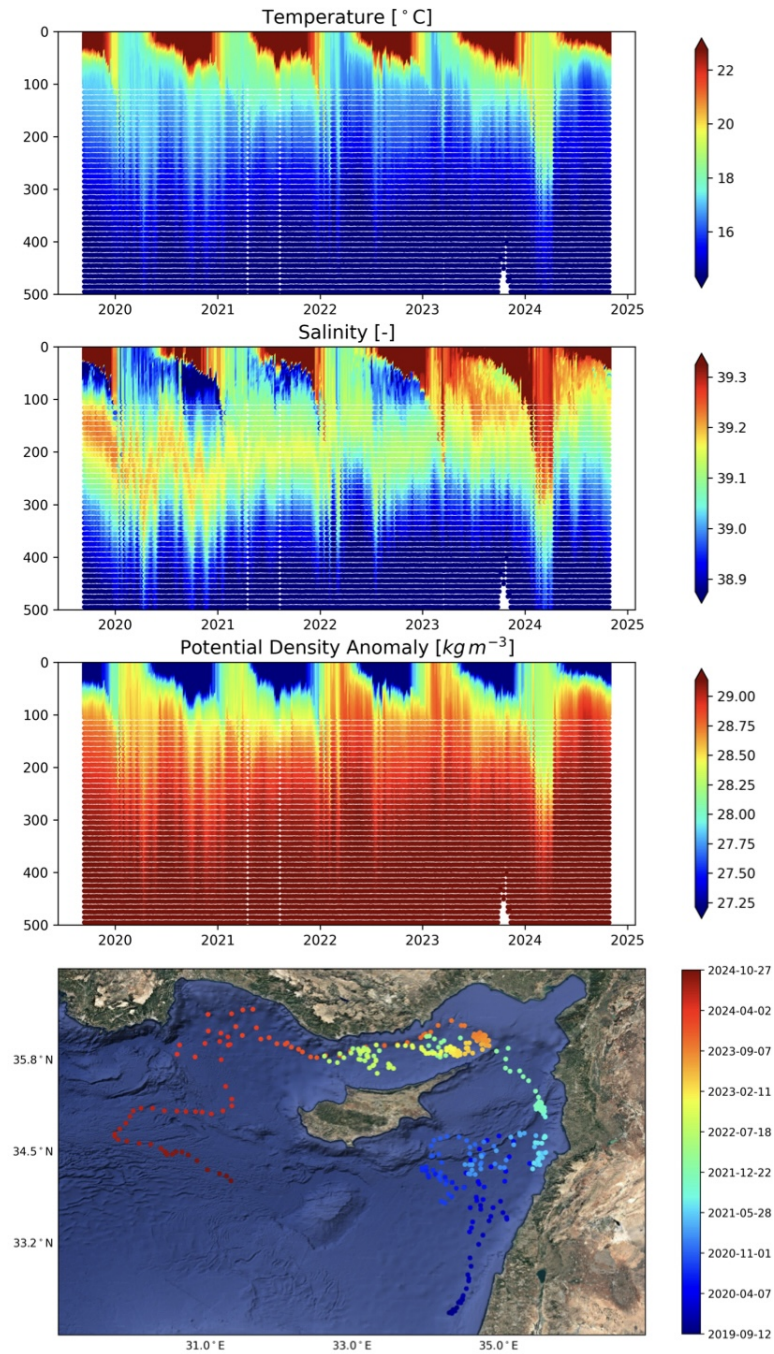


Figure 3. Hovmöller diagram of T, S and PDA for WMO=6903269 in the Levantine basin (white dots and lines are due to gaps in the data set.), with its trajectory shown at the bottom (image background from ©Google Maps).

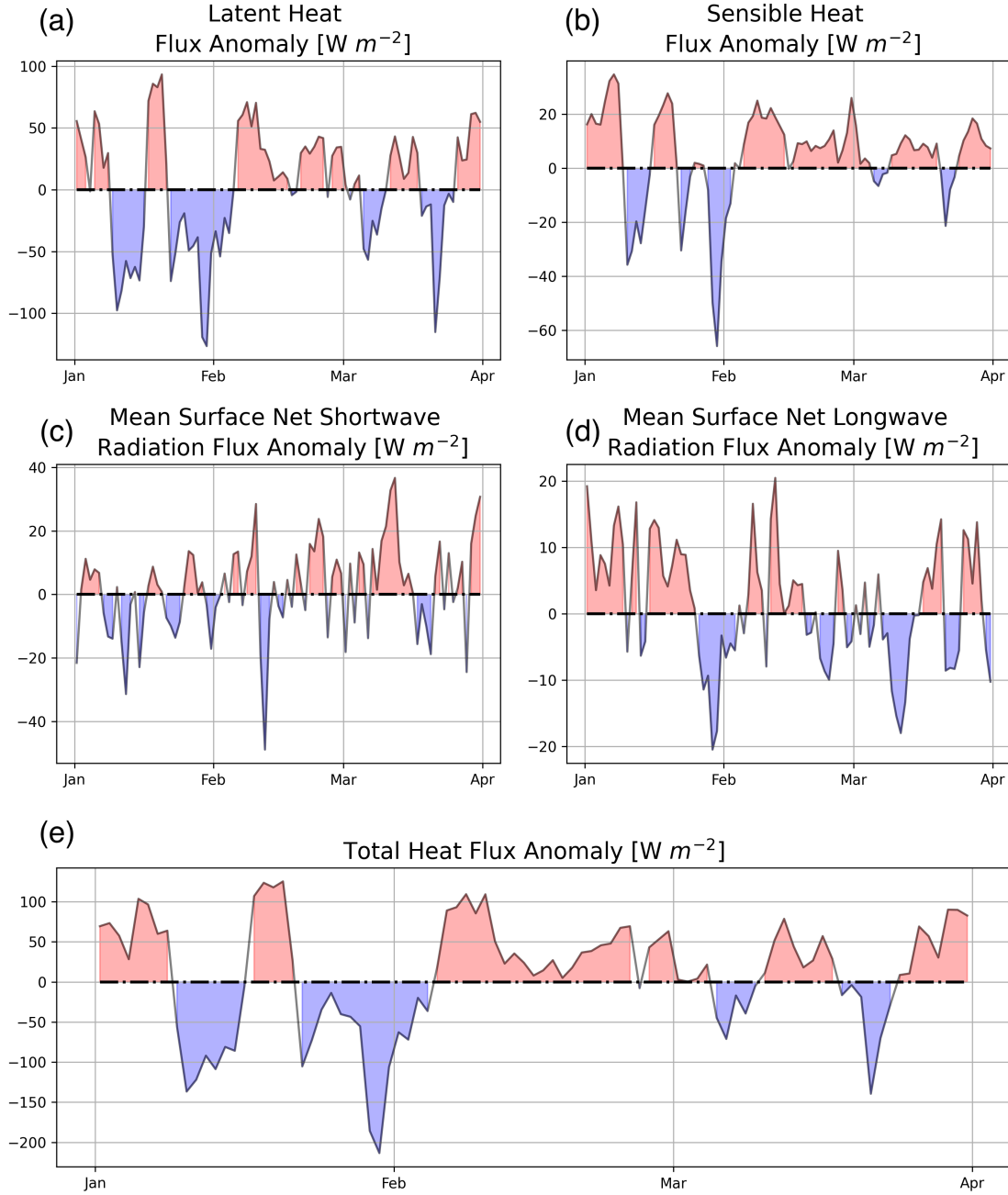


Figure 4. Daily ERA5 heat flux anomalies between 1 January and 1 April 2024 averaged over the Levantine basin with respect to the 2002–2024 climatology: (a) latent, (b) sensible, (c) net shortwave, (d) net longwave components and (e) the total sum.

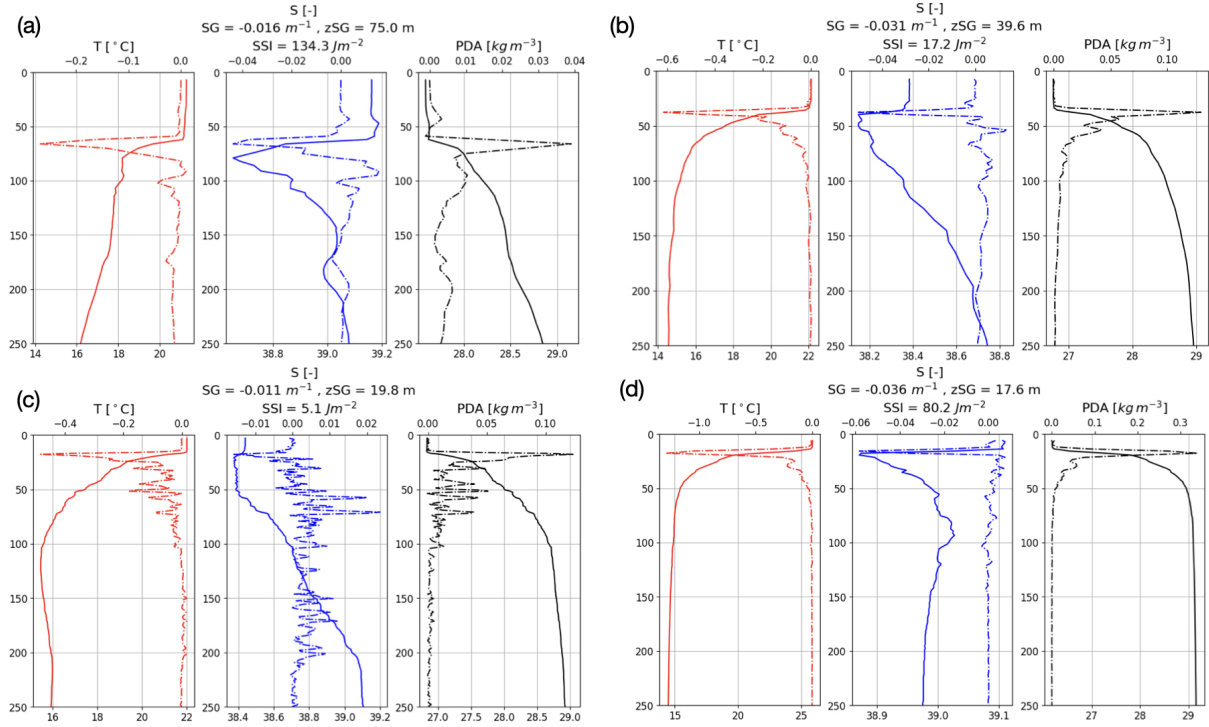


Figure 5. Examples of vertical T, S and PDA profiles (full lines) and their vertical rates of change (dashed lines) during which a surface saline lake is detected: a) the Levantine basin (float number 6901897, profile sampled in 28 November 2014), b) the Western Mediterranean (float number 6903820, profile sampled in 15 October 2024), c) the Ionian Sea (float number 6990629, sampled in 02 July 2024) and d) the Adriatic Sea (float number 6903799, sampled in 17 August 2023).

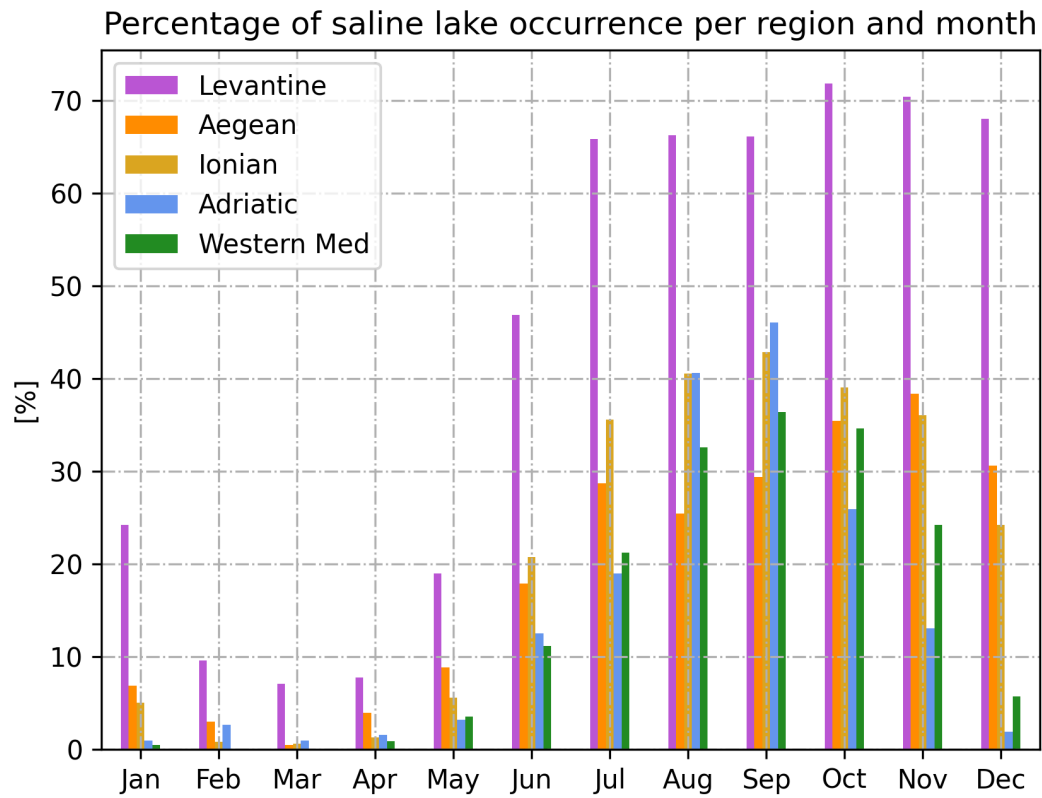


Figure 6. Percentages of profiles in which surface saline lakes occur for all months and basins.

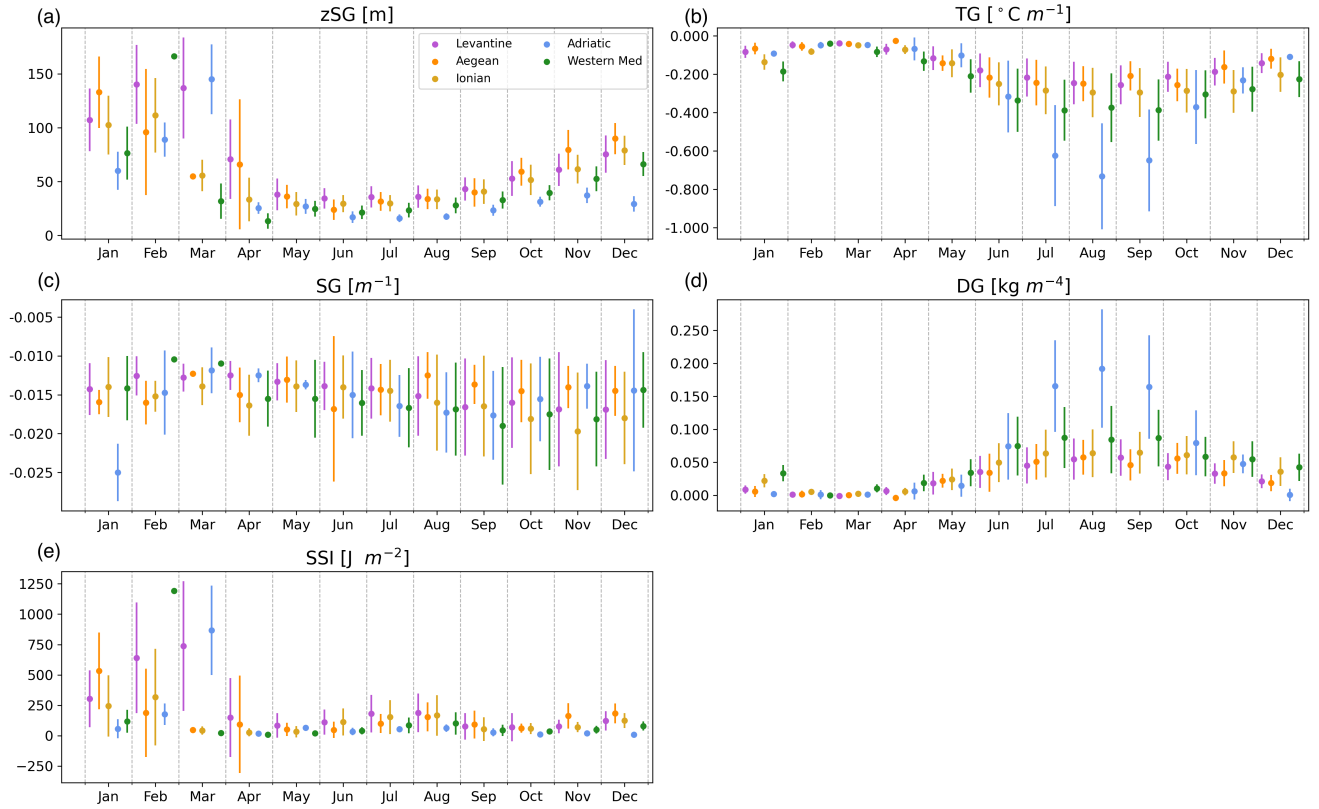


Figure 7. Monthly median and interquartile ranges (25-th and 75-th percentiles) in (a) the depth of surface saline lakes zSG , the respective (b) TG , (c) SG and (d) DG at the base of the lake, and (e) SSI of a lake over the selected regions.

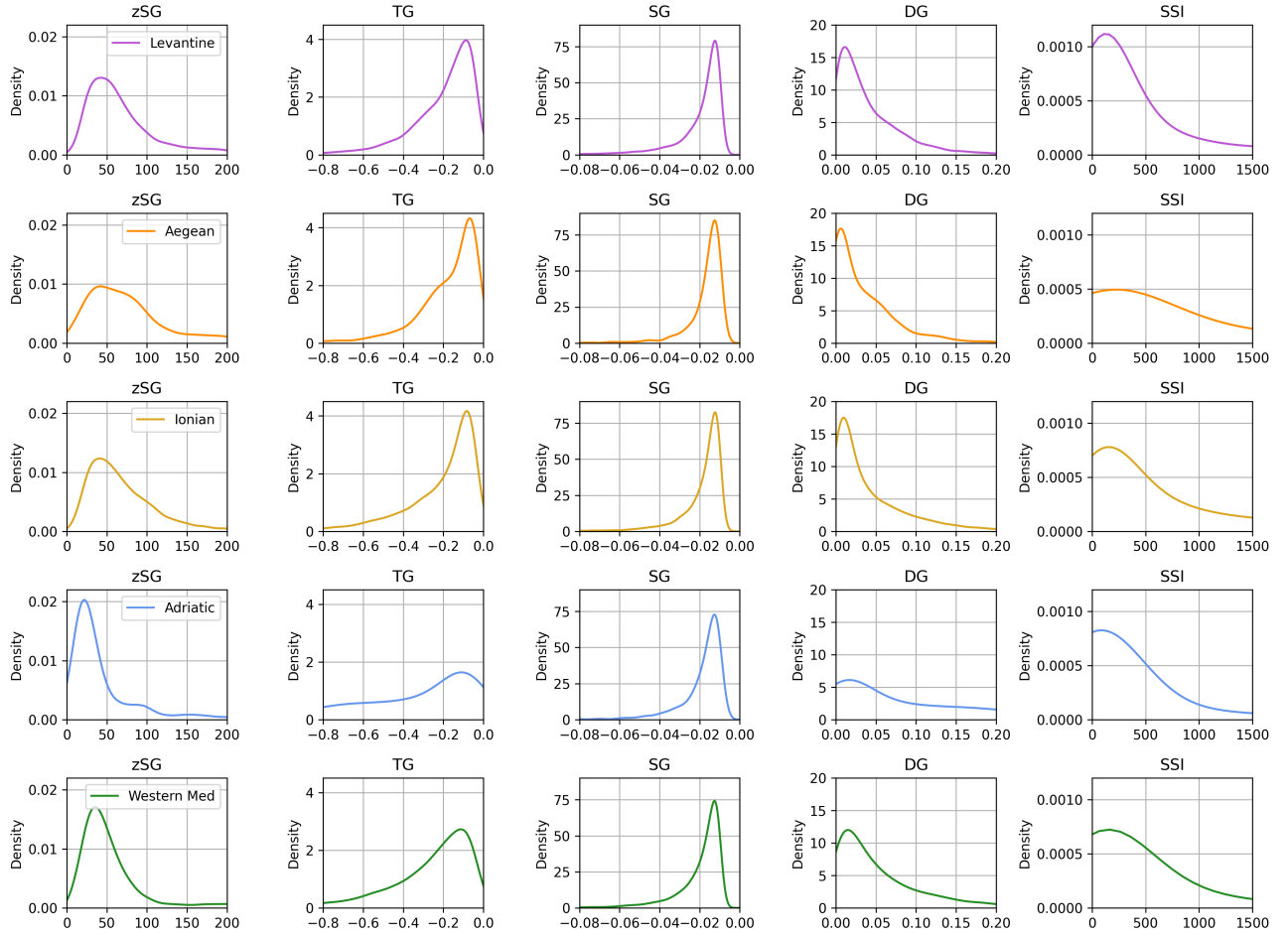


Figure 8. Probability density functions for: zSG , TG , SG , DG and SSI (columns) of a lake over the selected regions (rows).

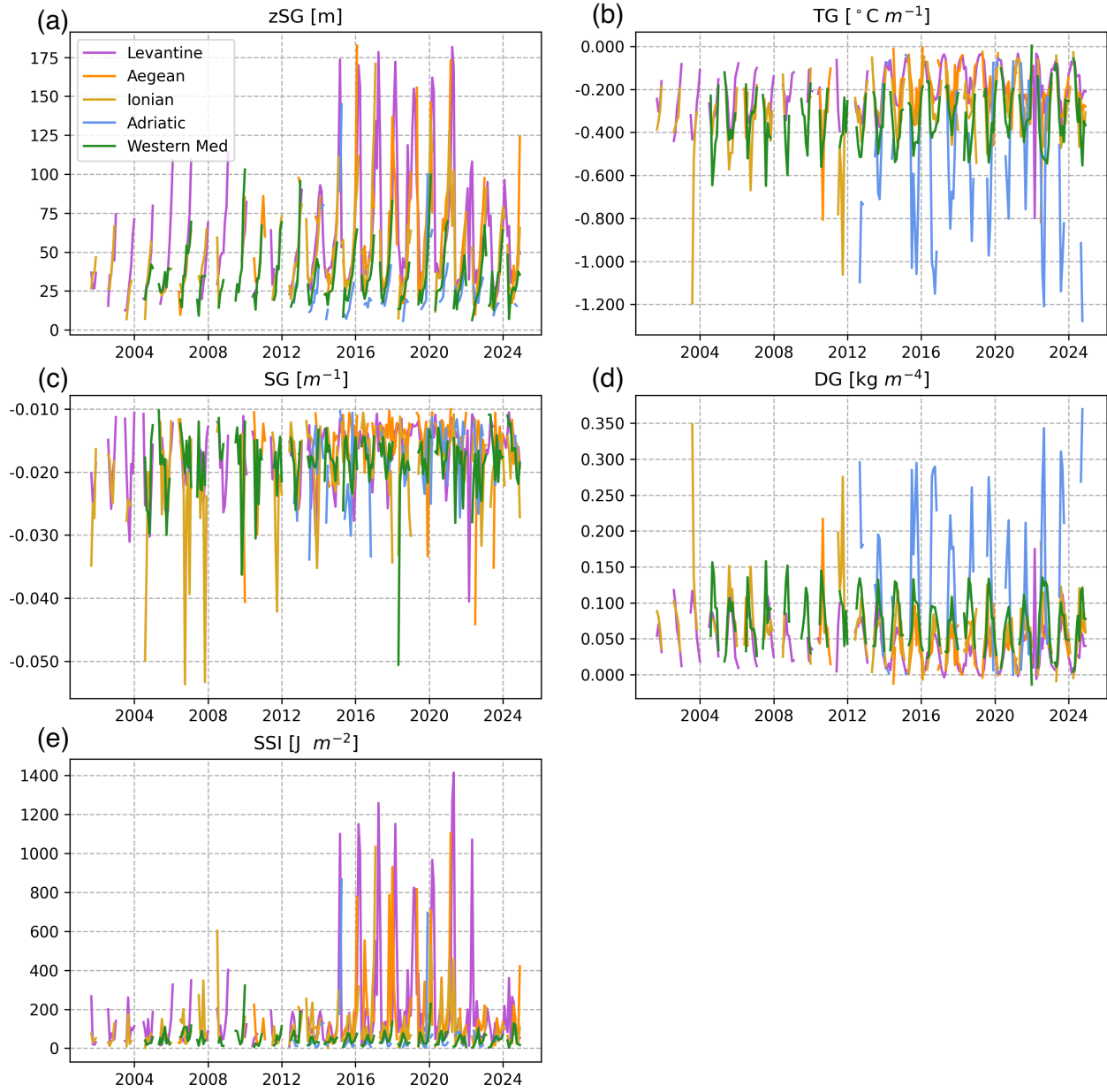


Figure 9. Monthly median time series in (a) the depth of surface saline lakes zSG , the respective (b) TG , (c) SG and (d) DG at the base of the lake, and (e) SSI of a lake over the selected regions.

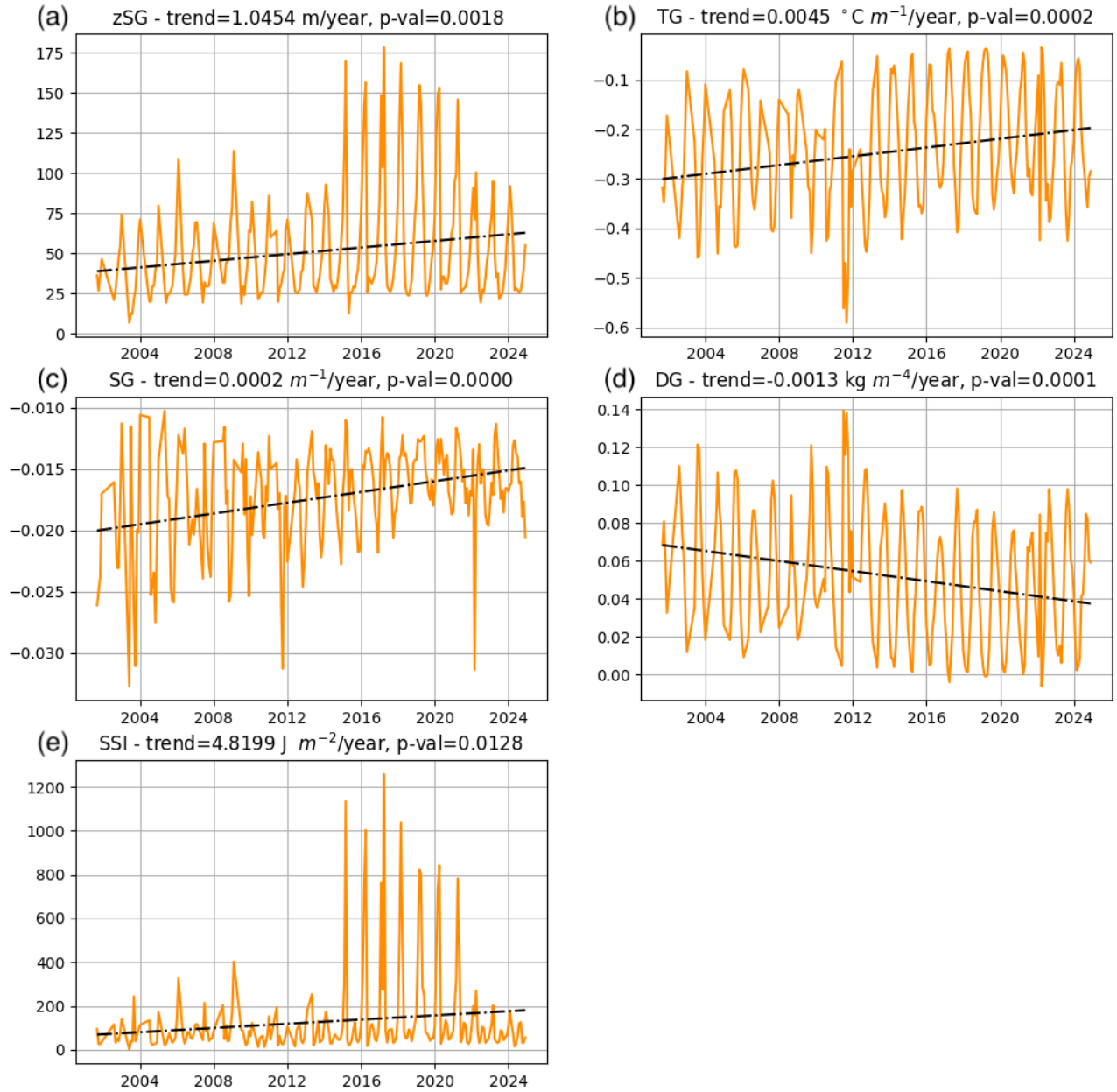


Figure 10. Linear trends in (a) the depth of surface saline lakes zSG , the respective (b) TG , (c) SG and (d) DG at the base of the lake, and (e) SSI of a lake.

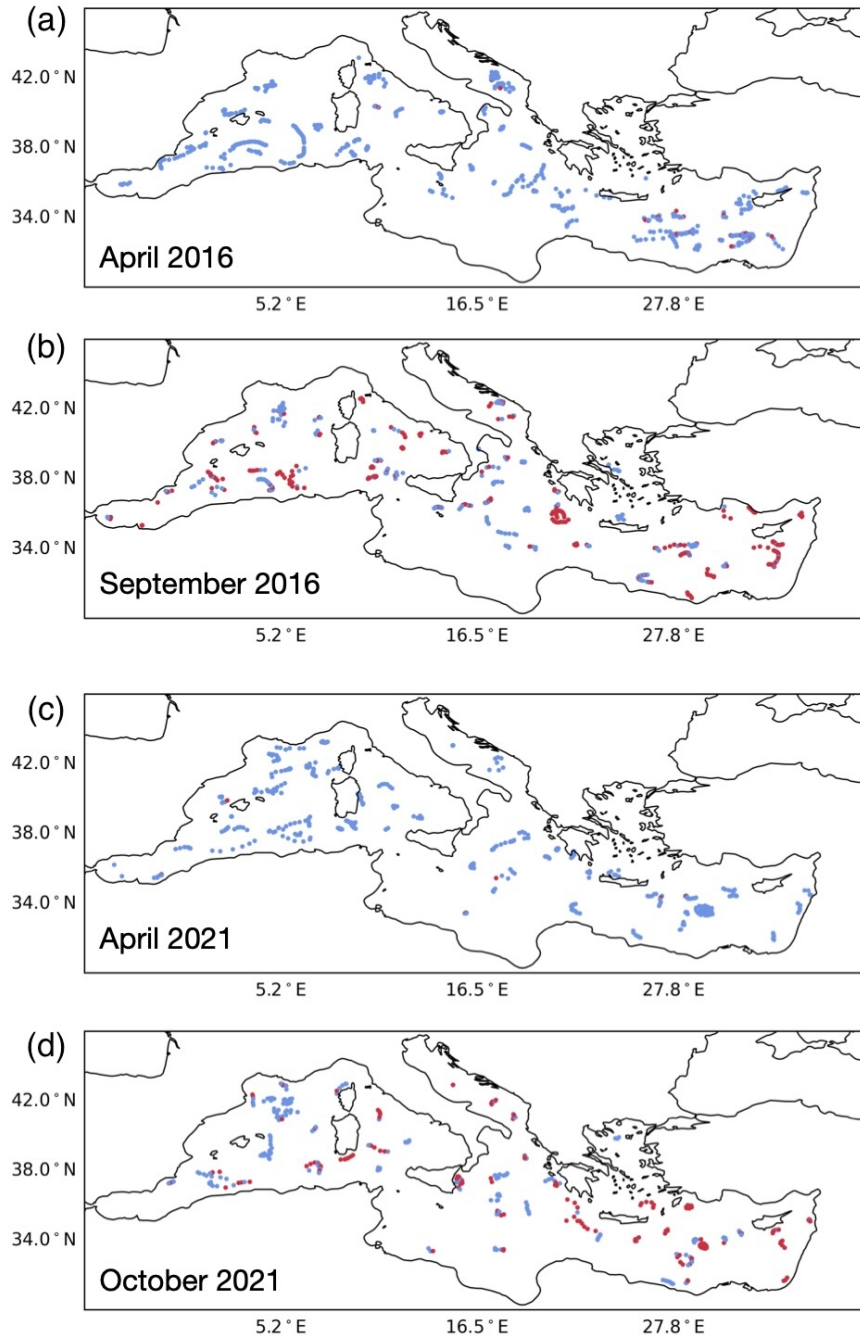


Figure 11. Examples of the spatial extent of SSLs over a certain month for: (a) April 2016, (b) September 2016, (c) April 2021 and (d) October 2021. Blue dots denote profiles without SSLs, whereas red ones highlight profiles with SSLs.